

Operating a Battery in a Hydropower-Dominated System to Balance Net Load Deviations

¹Christian Øyn Naversen, ¹Sigurd Bjarghov, ²Arild Helseth

¹Department of Electric Power Engineering, NTNU – Trondheim, Norway

²Department of Energy Systems, SINTEF Energy Research – Trondheim, Norway

Email: christian.naversen@ntnu.no, sigurd.bjarghov@ntnu.no, arild.helseth@sintef.no

Abstract— Decreasing costs of battery storage technologies make them a viable option for providing flexibility in power systems. In this paper, we study the operations of a battery in combination with cascaded hydropower in a system with uncertain net load due to wind power production. By simulating the operations of the combined system for a whole year by solving daily stochastic planning and real-time balancing problems, we show that the battery is only used when the hydropower system is under stress from large amounts of inflow and limited available storage capacity. The annual cost savings of adding the battery, including battery degradation costs, is 3,314 €, which is low compared to the investment costs of the battery. Since the inflow to the system follows a predictable seasonal pattern, the system operator should consider renting the battery storage from external sources, such as electric vehicles, instead of investing in a permanent battery.

Keywords—Rolling horizon simulator, Hydropower scheduling, System balancing, Battery degradation

I. INTRODUCTION

The amount of power produced from variable renewable sources is increasing quickly across the world, which increases the need for flexible balancing resources in power systems. Today, the Norwegian power system is dominated by hydropower, which is cheap and flexible compared to thermal generation. It is, therefore, a useful balancing resource, but the increased strain on the hydropower in the future system may require alternative balancing sources. Rapidly decreasing costs of Li-ion batteries make them a potential candidate in this regard.

The inclusion of batteries in systems with traditional thermal generation and renewable generation have been studied in detail in the literature. The role of battery storage devices is usually to balance out the mismatch in consumption and generation caused by increased renewable penetration [1]. Stochastic security constrained unit commitment (SSCUC) models, including a unit commitment stage and a balancing stage, are typically used to show the benefit of adding energy storage to such systems [2]–[4]. Pozo et al. present a general SSCUC formulation for the integration of energy storage in large scale systems in [2], including a linear cost for using the batteries. The value of the stochastic solution for thermal systems with energy storage and uncertain wind power was quantified in [3], which ranged from 0.5% to 4% depending on the level of wind power penetration. A way of calculating the system cost reduction of including energy storage was shown in [4], where the SSCUC solution was benchmarked by performing a deterministic rolling-horizon simulation of the real-time balancing problem. The cost savings were found to be around 13% based on six representative days. The model described in [5] finds a 2.3% - 7.8% cost reduction

using energy storage to avoid load shedding penalties, and the contingency constrained unit commitment model presented in [6] was used to show how energy storage can help stabilize the power system after a contingency event, such as a line outage, occurs. The stochastic economic dispatch model proposed in [7] for a joint wind power and battery operator demonstrates the economic benefit of including degradation costs in the optimization to avoid overuse of the battery.

Batteries and hydropower are two energy storage technologies governed by different dynamics. Batteries typically have a high installed power capacity relative to their storage potential. Running a full charge and discharge cycle can be accomplished within hours, resulting in what we will refer to as "fast dynamics". However, deep charging cycles does impact the life expectancy of battery due to quicker degradation. Hydropower plants often have a much larger storage capacity relative to installed power compared to batteries. Some hydropower reservoirs may take several years to empty, which makes the long-term planning of the reservoir storage levels a crucial factor in their scheduling. The seasonal changes in natural water inflow from melting snow and precipitation accentuate the importance of a long-term reservoir strategy. The slow dynamics of the hydropower system does not mean it is slow to react in the short-term, but that the flexibility of the system varies over the seasons.

The main contribution of this paper is the examination of the short-term and long-term dynamics of a combined hydropower and battery system considering battery degradation costs and net load uncertainty. A rolling horizon simulator was created for this purpose, consisting of a stochastic daily planning model and a stochastic real-time balancing model with a receding horizon. Section II describes the battery degradation formulation as well as the two optimization models. The simulation was performed for a Norwegian hydropower system described in Section III, and the results from comparing simulations with and without a battery are presented in Section IV. Concluding remarks are given in Section V.

II. MODEL

This section covers the basic building blocks of the simulator framework described in Section III. Section II-A describes the battery degradation formulation considered in this paper. The optimization models depicted in Sections II-B and II-C define problem formulations for the daily planning problem and the real-time balancing problem, respectively.

A. Battery degradation cost

The battery degradation cost is modelled as a piecewise linearized cost function for discharging the battery, as

proposed in [8]. The battery discharge variable is divided into N segments with an increasing degradation cost for increasing segment number i . The basis of the degradation cost calculation is the stress function Φ :

$$\Phi(\delta) = \frac{1}{N^{FEC}} \delta^2, \quad (1)$$

where δ is the relative cycle depth and N^{FEC} is the rated number of full equivalent cycles over the lifetime of the battery. The stress function represents the lifetime loss of performing a cycle of depth δ . As shown in Figure 1 for $N^{FEC} = 2,000$, the cycle life loss is 0.05% when performing a full cycle, but only 0.025% when performing a 70% cycle, resulting in a much lower cycle life cost per MWh for the shallow cycles. The linearized cost of using a discharge segment is based on how many cycles of that depth the battery can perform over its lifetime:

$$C_i^{bat} = \frac{C^{rep}}{\eta^{bat} E^{max}} N \left(\Phi \left(\frac{i+1}{N} \right) - \Phi \left(\frac{i}{N} \right) \right). \quad \forall i \in \mathcal{I} \quad (2)$$

The accuracy of the degradation cost function increases with the number of segments, as reflected in Figure 1. The strength of this approach is that the cycle depth dependency of degradation costs are well described so that the optimization model will refrain from heavy cycling.

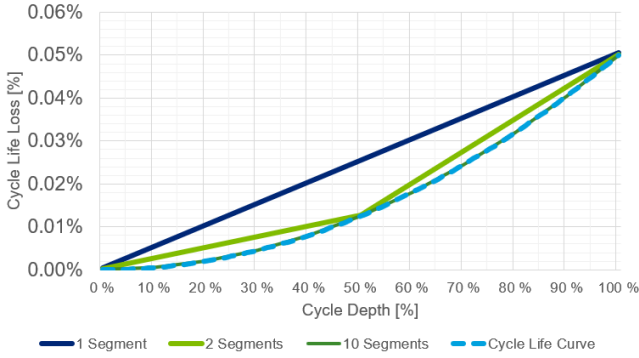


Fig. 1. Battery cycle depth stress function for $N^{FEC} = 2,000$ with three piece-wise linear approximations.

B. Daily planning problem

The daily planning problem takes the perspective of a system operator responsible for finding the production schedules, reserve capacity allocation, and external market position that meets the forecasted net load and is expected to give the lowest balancing costs in real-time operations. The net load forecast is uncertain due to the presence of wind power generation in the system, which is implicitly modelled through the net load. The external market is used to model the interaction with connected areas that are not explicitly modelled. It is formulated as a step function with different offers for buying and selling power for the next day. The planning problem is a two-stage stochastic program, where the second stage is the balancing stage after net load uncertainty has been realized. First, let the deterministic hydropower and battery scheduling problem be denoted as

$$\min_{\mathbf{x} \in \mathcal{X}} Z(\mathbf{x}), \quad (3)$$

with all variables contained in the vector \mathbf{x} , all constraints described by $\mathbf{x} \in \mathcal{X}$, and the objective function $Z(\mathbf{x})$. The main components of this problem are defined as:

$$\min_{\substack{a, v, p, u \\ q^{in}, q^d, q^b \\ e, c, d}} \left\{ a + \sum_{t \in \mathcal{T}} F_t \left(C^b \sum_{m \in \mathcal{M}} q_{mt}^b + \sum_{k \in \mathcal{K}} C_k^{mark} u_{kt} \right) + \sum_{t \in \mathcal{T}} F_t \sum_{i \in \mathcal{I}} C_i^{bat} d_{it} \right\} \quad (4)$$

$$a \geq B_l - \sum_{m \in \mathcal{M}} W V_{ml} v_{m, T+1} \quad \forall l \in \mathcal{L} \quad (5)$$

$$q_{mt}^{in} = I_{mt} + \sum_{j \in \mathcal{J}_m^d} \sum_{n \in \mathcal{N}_j} q_{jnt}^d + \sum_{j \in \mathcal{J}_m^b} q_{jt}^b \quad \forall m, t \in \mathcal{M}, \mathcal{T} \quad (6)$$

$$\frac{v_{m, t+1} - v_{mt}}{F_t} = q_{mt}^{in} - q_{mt}^b - \sum_{n \in \mathcal{N}_m} q_{mnt}^d \quad \forall m, t \in \mathcal{M}, \mathcal{T} \quad (7)$$

$$\frac{e_{t+1} - e_t}{F_t} = \eta^{bat} c_t - \sum_{i \in \mathcal{I}} d_{it} \quad \forall t \in \mathcal{T} \quad (8)$$

$$p_{mt} = \sum_{n \in \mathcal{N}_m} \eta_{mn}^d q_{mnt}^d \quad \forall m, t \in \mathcal{M}, \mathcal{T} \quad (9)$$

$$\sum_{m \in \mathcal{M}} p_{mt} + \eta^{bat} \sum_{i \in \mathcal{I}} d_{it} - c_t = L_t - \sum_{k \in \mathcal{K}} u_{kt} \quad \forall t \in \mathcal{T} \quad (10)$$

In addition to eqs. (4)-(10), initial volume and energy constraints as well as variable bounds are also included in the constraints for model (3). The hydropower scheduling formulation used here is a standard formulation, see for instance [9], specifically eqs. (7)-(11) in Section 3.2. The objective (4) is the expected future cost of the hydropower system in addition to the current costs of using the battery, bypass gates and trading in the external market. The battery degradation cost segments are calculated a priori based on eq. (2). The expected future cost of the hydropower system is described by the Benders cuts in eq. (5), which can be calculated by long-term hydropower scheduling models such as [9]. The cut description is a way of propagating the long-term reservoir management strategy of the hydropower system to the short-term scheduling problem. The hydropower topology and reservoir balance are accounted for in eqs. (6) and (7), while the energy balance of the battery is described in eq. (8). Equation (9) is the water-to-power conversion function for the hydropower modules. Finally, eq. (10) enforces the power balance in the system. The deterministic problem schedules the production and consumption of the battery and hydropower modules to meet the expected net load and any additional volumes bought or sold in the external market, while minimizing the system costs.

To account for the net load uncertainty, the system operator also procures spinning reserve capacity on the hydropower modules according to eq. (11):

$$r_{mt} \leq p_{mt} \leq P_m^{max} - r_{mt}. \quad \forall m, t \in \mathcal{M}, \mathcal{T} \quad (11)$$

The reserve capacity is required to be symmetric in eq. (11) to make sure the turbines delivering the capacity are spinning. Including binary variables and minimum production limits

on the hydropower would allow for an asymmetric reserve capacity allocation, but the tractability of the linear problem is preferred in the simulator setup described in Section III. A two-stage stochastic problem extension of the deterministic problem is formulated to model the cost of balancing the system in real-time. The first-stage problem is identical to eqs. (4)-(11), denoted by model (3). The second-stage problem is defined for each net load scenario $s \in \mathcal{S}$ and contains the variables \mathbf{y}_s , which are scenario specific copies of the variables found in \mathbf{x} . The only connection between the two stages is the hydropower production limits

$$\begin{aligned} \bar{p}_{smt} &\leq p_{mt} + r_{mt} & \forall s, m, t \in \mathcal{S}, \mathcal{M}, \mathcal{T}, \\ \bar{p}_{smt} &\geq p_{mt} - r_{mt} & \forall s, m, t \in \mathcal{S}, \mathcal{M}, \mathcal{T}, \end{aligned} \quad (12)$$

and the nonanticipativity constraints for the market position in all scenarios:

$$\bar{u}_{skt} = u_{kt} \quad \forall s, k, t \in \mathcal{S}, \mathcal{K}, \mathcal{T}. \quad (13)$$

Note that the scenario specific variables \mathbf{y}_s have been denoted with an overline to separate them from their first-stage counterparts. The two-stage problem can now be written as

$$\min_{\mathbf{x}, \mathbf{y}_s} Z(\mathbf{x}) + \sum_{s \in \mathcal{S}} \pi_s Z(\mathbf{y}_s) \quad (14)$$

$$\mathbf{x} \in \mathcal{X} \quad (15)$$

$$\mathbf{y}_s \in \mathcal{Y}_s(\mathbf{x}) \quad \forall s \in \mathcal{S}, \quad (16)$$

where the spinning reserve variables r_{mt} and eq. (11) have been added to \mathbf{x} and \mathcal{X} , respectively. The second-stage constraints, described by eq. (16), includes scenario specific copies of eqs. (5)-(10), and eqs. (12) and (13). The cost functions for the first and second stage has the same functional expression as shown in eq. (4), and the scenario probabilities π_s are used to weight the second-stage cost. The stochastic problem aims at scheduling production and consumption to cover the forecasted net load, in addition to procure reserve capacity to cover all net load scenarios.

C. Real-time balancing problem

The real-time balancing of the system is modelled by a two-stage receding horizon stochastic program, which is based on the solution of the planning stage model described in Section II-B. The external market position cannot be renegotiated in real-time, and is fixed in all scenarios according to eq. (13). The same is true for the procured reserve capacity, and so the upper and lower hydropower production bounds are fixed by eq. (12). The fixed planning stage decisions are denoted by \mathbf{x}^* . The net load uncertainty is realized in hourly steps, and the optimal way to balance the system given a set of net load scenarios for the remaining hours is found by solving eqs. (17)-(19):

$$\min_{\mathbf{y}_s} \sum_{s \in \mathcal{S}} \pi_s Z(\mathbf{y}_s) \quad (17)$$

$$\mathbf{y}_s \in W(\tau) \quad \forall s \in \mathcal{S} \quad (18)$$

$$\mathbf{y}_s \in \mathcal{Y}_s(\mathbf{x}^*) \quad \forall s \in \mathcal{S}, \quad (19)$$

The time τ represents the latest hour where the net load is known, which is initially $\tau = 1$. The constraints defined in eq. (18) represent fixing all time-dependent variables for $t < \tau$

as well as the nonanticipativity constraints of eqs. (6)-(10) in hour τ where the net load has just been realized. The problem is initially solved for $\tau = 1$ and is then subsequently re-solved for $\tau \rightarrow \tau + 1$ until $\tau = T$ and the uncertainty in all hours has been realized.

III. CASE STUDY

A rolling horizon simulator scheme based on the daily planning problem in Section II-B and the real-time balancing problem in Section II-C is used to simulate the impact of adding a battery in a hydropower-dominated system. The total time horizon of the simulator is set to 52 weeks, where every day is solved in succession. This setup captures the fast dynamics involved in balancing the system hour by hour, as well as the long-term reservoir management aspects of hydropower scheduling. First, the stochastic planning model, eqs. (14)-(16), is solved for the next day with hourly time resolution. The solution from this model is then used in the real-time balancing problem, eqs. (17)-(19), which simulates the operations of the system as the net load uncertainty is realized in hourly steps. The time resolution in the realized hours is 5 minutes, while hourly time resolution is used for the remainder of the horizon. The end volume of the hydropower reservoirs and the final energy content of the battery at the end of each day is carried over to form the initial conditions for the following day. The simulator logic is shown in Figure 2.

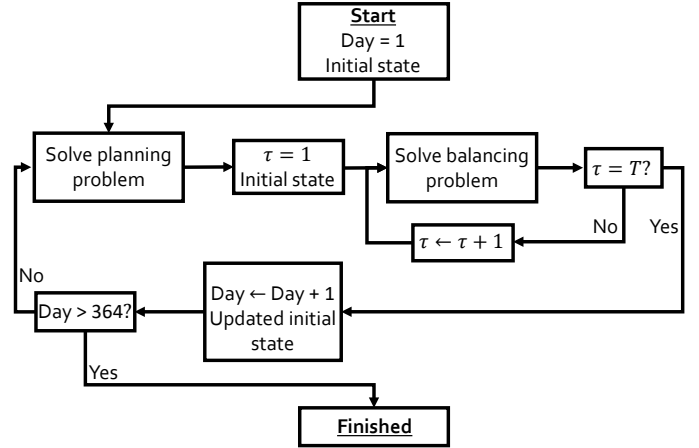


Fig. 2. A simplified flowchart of the 52 week simulator. The daily planning problem and real-time balancing problem are solved for each day in the period.

The hydropower topology used in this case study is based on a real cascaded system from the middle of Norway, which contains 12 connected hydropower modules in a cascaded configuration. The system includes large reservoirs capable of storing several hundred Mm^3 of water as well as a river string of reservoirs that can be drained within hours. The initial reservoir content of every reservoir is set to 60% of their maximal storage capacity at the start of the simulation. Benders cuts for each of the 52 weeks were generated by the long-term hydropower scheduling model described in [9] as input to the simulation.

The parameters used to model the battery is included in Table I. The battery size of 10MW and 10MWh was chosen after performing test runs with different sizes. The efficiency of charging and discharging were set to $\eta^{bat} = 97\%$, resulting in a round-trip efficiency of 94.09%. The replacement cost

TABLE I. BATTERY PARAMETERS.

Battery parameter	Symbol	Value
Storage capacity	E^{max}	10 MWh
Max charging power	D^{max}	10 MW
Max discharging power	D^{max}	10 MW
Efficiency	η^{bat}	97%
Full equivalent cycles	N^{FEC}	2,000
Battery replacement cost	C^{rep}	75,000 €/MWh

of the battery was assumed to be 75,000 €/MWh. Both the efficiency and the replacement cost represent an optimistic future outlook for the development of battery technology. Ten equally spaced segments were used in the linearization of the battery degradation model. The total number of full equivalent battery cycles during the lifetime of the battery was set to $N^{FEC} = 2,000$.

The net load uncertainty represents the forecast errors in wind power production in the system. As a first-order approximation of this uncertainty, the net load scenarios used by both the daily planning problem and the real-time balancing problem were randomly generated by drawing from a normal distribution $N(\mu, \sigma)$ for each hour of the simulator horizon. The expected value μ was set to equal the forecasted net load L_t , while the standard deviation was calculated as 10% of the forecasted peak load for the given day. Any number drawn from this distribution outside $L_t \pm 2.5\sigma$ was truncated, which represents the maximal deviations possible for the installed wind power. Ten scenarios with hourly resolution were generated based on the normal distribution for the entire simulator time horizon of 52 weeks. In addition, two scenarios with values of $L_t + 2.5\sigma$ and $L_t - 2.5\sigma$ were added to serve as the extreme balancing cases. The probabilities of each extreme scenario were set to 2.5%, while the generated scenarios all have an equal probability of 9.5%. The realized net load was also generated from the same normal distribution as the scenarios, but additional deviations for each 5-minute interval was added from the normal distribution $N(0, 2)$. The values of the realized net load were truncated in the same manner as the scenarios, ensuring that the realized net load always stays within the bounds of the two extreme scenarios. This ensures that no load shedding or power spilling occurs in the real-time balancing problem, which could otherwise have a large impact on the numerical results shown in Section IV.

The external market step curve was created with offers of both buying and selling power at prices ranging from 50 to 5 €/MWh. It is possible to buy an unlimited amount of power for 50 €/MWh, and power can similarly always be sold for 5 €/MWh. These values cap the system prices seen in the daily planning problem, but higher and lower prices can be experienced in the real-time balancing problem since the external market position is fixed.

IV. RESULTS

The case study described in Section III was run twice, with and without the battery included in the system. Table II shows the breakdown of the change in costs when the battery was added. The total system cost is reduced by 3,314 € over the 52 simulated weeks, and most of the savings come from a lower future expected system cost at the end of the year. A more beneficial distribution of the water among the reservoirs, as well as 0.17 Mm³ of additional water being stored in the

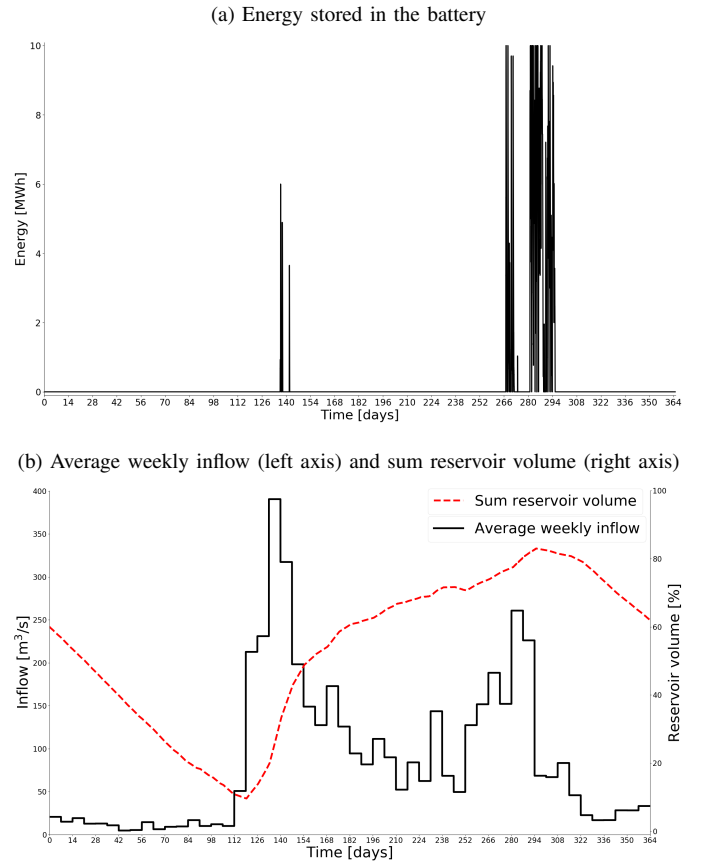


Fig. 3. The battery usage shown in a) depends on the hydrological situation in the hydropower system shown in b).

system at the end of the 52 weeks, are the causes of the lower expected future costs.

TABLE II. CHANGE IN SYSTEM COSTS WHEN A BATTERY IS ADDED TO THE SYSTEM.

Type of cost	Change when battery is present
Net external market cost	-1,090 €
Bypass cost	-63 €
Battery degradation cost	+1,013 €
Future expected system cost	-3,174 €
Total	-3,314 €

The cost savings of including the battery in the system represents a 0.44% return on the 750,000 € battery investment cost. Investing in the battery does not constitute a good investment for the system operator based on this simulation. However, Figure 3 shows that there is a strong correlation between the use of the battery and the hydrological situation in the hydropower system. The battery is only used to store energy during the spring flood and the wet weeks of autumn, as this is the period when the hydropower system is constrained the most. The inflow peak in the spring is not as critical in this simulation, as most of the reservoirs have low water levels after the winter and can store most of the inflow. The situation is more precarious in the autumn when many of the reservoirs are full of water. The hydropower plants must operate at a high capacity to discharge the water out of the system when the reservoirs are full and the inflow is high, but the uncertain net

load forces many of the hydropower plants to operate below maximum capacity. The alternative to discharging the water through the turbines is to use the bypass gates at the cost of a small penalty C^b and lost potential power production. The inclusion of the battery helps to shift some of the balancing responsibility away from the hydropower plants, which lets them operate at a higher capacity instead of bypassing water. The battery is only needed for 18 days (5%) of the year, and only during the predictable high inflow weeks. The flexibility and cost of the hydropower outperforms the battery for the rest of the year, even in sub-hourly system balancing. Instead of investing in a stationary battery, the system operator could use electric vehicles or other local battery storage options to reduce the system costs during the specific weeks in question.

V. CONCLUSION

This paper investigates the impact of a large-scale battery considering cycle ageing in a cascaded hydropower-dominated system under net load uncertainty. For this purpose, we created a rolling horizon simulator that aims at minimizing the immediate operational system costs as well as optimizing the long-term use of the reservoir content. The simulator works by repeatedly solving a stochastic planning problem and a stochastic real-time balancing problem for each day of the simulator horizon.

Running the simulator over a whole year for a real Norwegian watercourse uncovered that the battery is used when the inflow to the hydropower reservoirs is high, and especially if the reservoir storage levels are close to maximal capacity. The battery is able to alleviate the hydropower in these situations, which leads to better water management. The cost savings of adding the battery was found to be 3,314 €, which is a poor investment considering the high cost of purchasing the battery. Instead, the system operator could consider renting distributed local storage for the 18 days during spring and fall that the battery is beneficial to the system.

Possible future work should look into the impact of inflow uncertainty in the model, as the operation of the battery is strongly linked to the hydrological situation in the hydropower system. Increasing the price volatility of the external market and the size of the deviations in the net load would likely lead to increased battery activity, which is not an unlikely future scenario in the Norwegian power system.

ACKNOWLEDGMENTS

This work was funded by The Research Council of Norway, Project No. 268014/E20.

REFERENCES

- [1] B. P. Roberts and C. Sandberg, "The Role of Energy Storage in Development of Smart Grids," *Proc. IEEE*, vol. 99, no. 6, pp. 1139–1144, jun 2011.
- [2] D. Pozo, J. Contreras, and E. E. Sauma, "Unit Commitment With Ideal and Generic Energy Storage Units," *IEEE Trans. Power Syst.*, vol. 29, no. 6, pp. 2974–2984, nov 2014.
- [3] R. Hemmati, H. Saboori, and S. Saboori, "Assessing wind uncertainty impact on short term operation scheduling of coordinated energy storage systems and thermal units," *Renew. Energy*, vol. 95, pp. 74–84, sep 2016.
- [4] N. Li, C. Uckun, E. M. Constantinescu, J. R. Birge, K. W. Hedman, and A. Botterud, "Flexible Operation of Batteries in Power System Scheduling With Renewable Energy," *IEEE Trans. Sustain. Energy*, vol. 7, no. 2, pp. 685–696, apr 2016.

- [5] A. Khazali and M. Kalantar, "Stochastic reserve scheduling in smart systems incorporating energy storage systems," in *2017 IEEE Int. Conf. Environ. Electr. Eng. 2017 IEEE Ind. Commer. Power Syst. Eur. (EEEIC / I&CPS Eur.)*. IEEE, jun 2017, pp. 1–6.
- [6] Y. Wen, C. Guo, H. Pandzic, and D. S. Kirschen, "Enhanced Security-Constrained Unit Commitment With Emerging Utility-Scale Energy Storage," *IEEE Trans. Power Syst.*, vol. 31, no. 1, pp. 652–662, jan 2016.
- [7] Y. Wang, Z. Zhou, A. Botterud, K. Zhang, and Q. Ding, "Stochastic coordinated operation of wind and battery energy storage system considering battery degradation," *J. Mod. Power Syst. Clean Energy*, vol. 4, no. 4, pp. 581–592, oct 2016.
- [8] B. Xu, J. Zhao, T. Zheng, E. Litvinov, and D. S. Kirschen, "Factoring the Cycle Aging Cost of Batteries Participating in Electricity Markets," *IEEE Trans. Power Syst.*, vol. 33, no. 2, pp. 2248–2259, 2018.
- [9] A. Helseth, B. Mo, A. Lote Henden, and G. Warland, "Detailed long-term hydro-thermal scheduling for expansion planning in the Nordic power system," *IET Gener. Transm. Distrib.*, vol. 12, no. 2, pp. 441–447, 2018.

NOMENCLATURE

Sets and indices

\mathcal{T}	Set of time steps, index t .
\mathcal{M}	Set of hydropower modules, index m .
\mathcal{S}	Set of net load scenarios, index s .
\mathcal{K}	Set of external market steps, index k .
\mathcal{L}	Set of Benders cuts, index l .
\mathcal{I}	Set of battery discharge segments, index i .
\mathcal{N}_m	Set of module discharge segments, index n .
$\mathcal{J}_m^{d/b}$	Set of modules that discharge/bypass water to module m , index j .

Parameters

η^{bat}	Battery efficiency [1].
η_{mn}^d	Hydropower efficiency [MW/m ³].
π_s	Scenario probability [1].
B_l	Constant term in Benders cuts [€].
C^b	Penalty cost for bypassing water [€/m ³].
C_i^{bat}	Degradation cost of the battery [€/MWh].
C_k^{mark}	Cost/income of buying/selling power in the external market [€/MWh].
C^{rep}	Battery replacement cost [€].
D^{max}	Maximal battery charging and discharging power [MW].
E^{max}	Maximal battery storage capacity [MWh].
F_t	Length of time step [s] or [h].
I_{mt}	Natural reservoir inflow [m ³ /s].
L_t	Net forecasted load [MW].
N	Number of battery discharge segments.
N^{FEC}	Number of full equivalent cycles during the lifetime of the battery.
P_m^{max}	Maximal hydropower production [MW].
T	Total number of time steps in \mathcal{T} .
WV_{ml}	Benders cut coefficient [€/m ³].

Variables

a	Future expected hydropower system cost [€].
v_{mt}	Reservoir volume [m ³].
p_{mt}	Hydropower production [MW].
r_{mt}	Spinning reserved hydropower capacity [MW].
u_{kt}	External market position [MW].
q_{mnt}^d	Discharge from hydropower [m ³ /s].
q_{mt}^b	Bypass from hydropower [m ³ /s].
q_{mt}^{in}	Total reservoir inflow [m ³ /s].
e_t	Energy content of the battery [MWh].
c_t	Battery charge [MW].
d_{it}	Battery discharge [MW].